Supporting Information

Sandwich-like NiCo-LDH/rGO with Rich Mesopores and High Charge Transfer Capability for Flexible Supercapacitors

Jiaqi Wang[1], Yuancong Luo[1], Lei Ling[1], Xue Wang[1], Shicong Cui[3], Zhen Li[2, *], Zheng Jiao[2], Lingli Cheng[1, *]

1. School of Environmental and Chemical Engineering, Shanghai University, Shanghai, 200444, P.R. China

2. Shanghai Applied Radiation Institute, Shanghai University, Shanghai, 201800, P.R. China

3. Department of Chemistry, East China University of Science and Technology, Shanghai, 200237, P.R. China

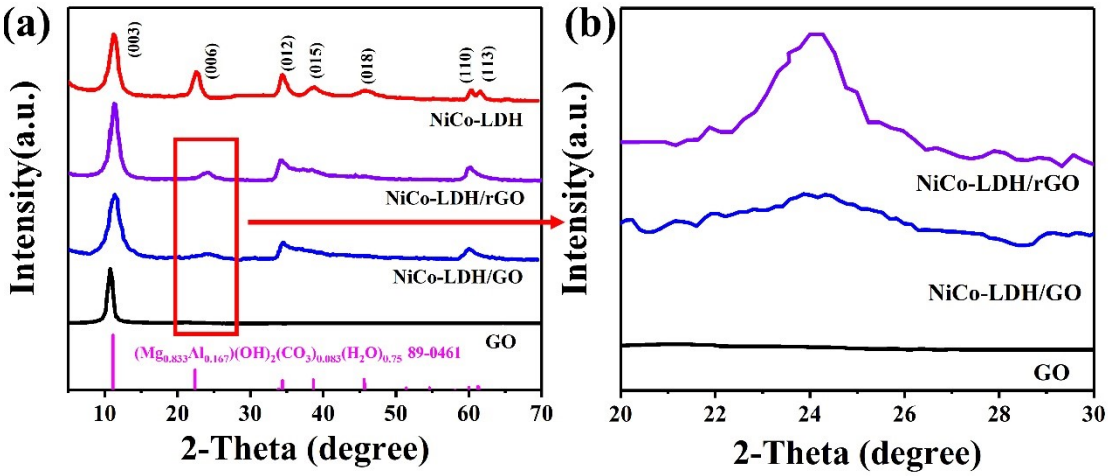

Figure S1. (a) XRD pattern of GO, NiCo-LDH, NiCo-LDH /GO and NiCo-LDH /rGO, (b) XRD pattern of GO, NiCo-LDH/GO, and NiCo-LDH/rGO.

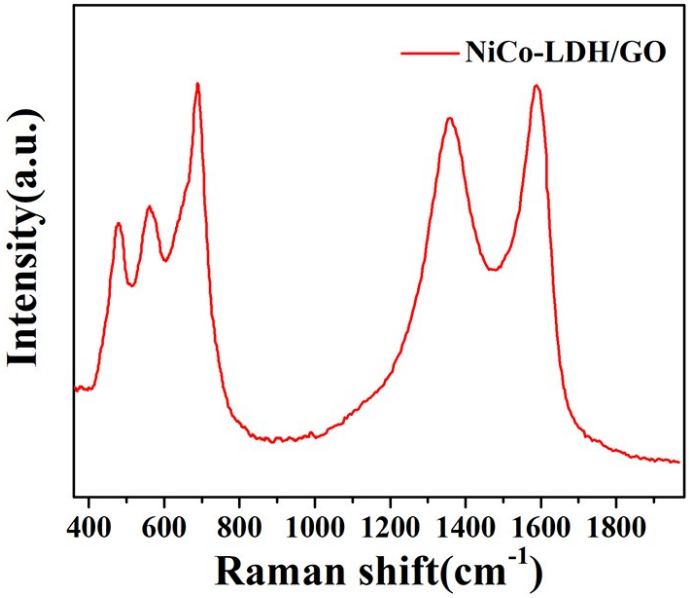

Figure S2. Raman spectra of NiCo-LDH/GO.

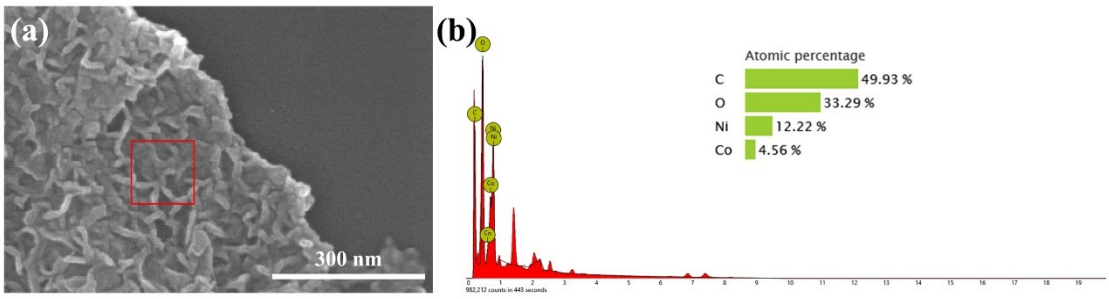

Figure S3. (a)(b)EDS mapping of NiCo-LDH/rGO

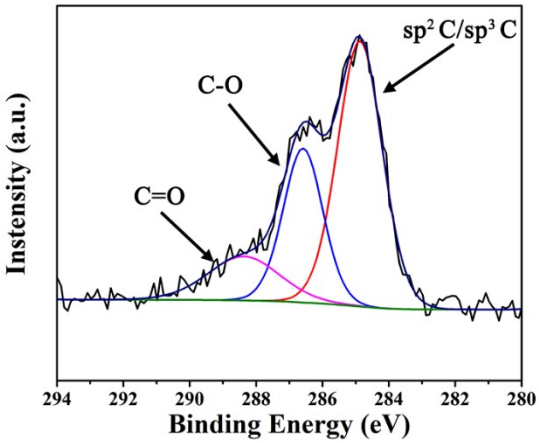

Figure S4. XPS spectra of C 1s for NiCo-LDH/GO.

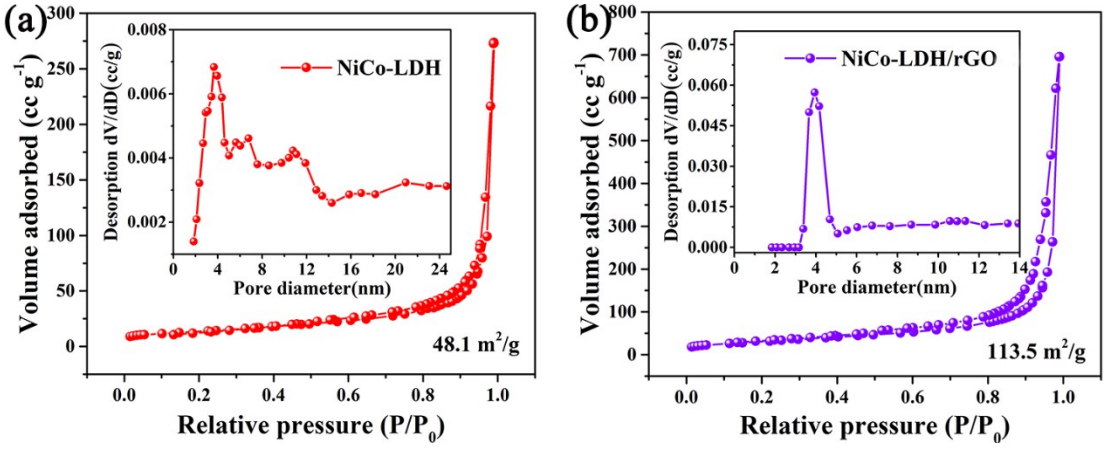

Figure S5. (a) N_2 adsorption/desorption isotherms of NiCo-LDH together with its pore size distributions (inset); (b) N_2 adsorption/desorption isotherms of NiCo-LDH/rGO together with its pore size distributions (inset).

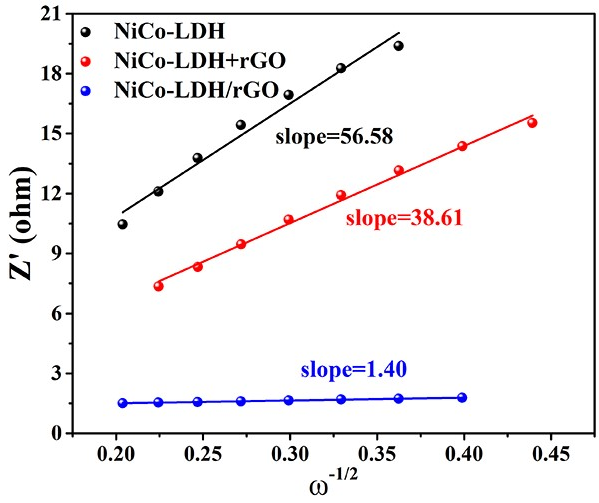

Figure S6. Z′ as a function of $\omega^{-1/2}$ plot in low frequency.

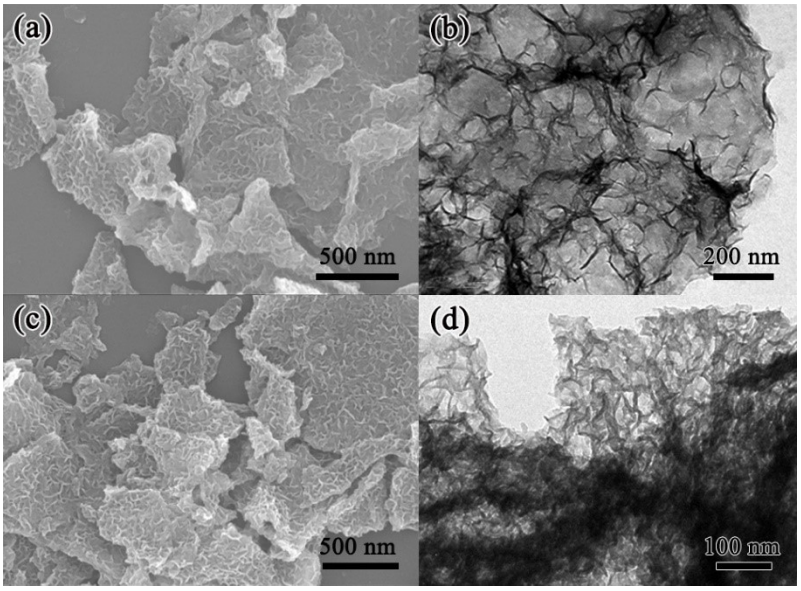

Figure S7. (a)(b)FESEM and TEM image of NiCo-LDH/rGO-1; (c)(d) FESEM and TEM image of NiCo-LDH/rGO-3.

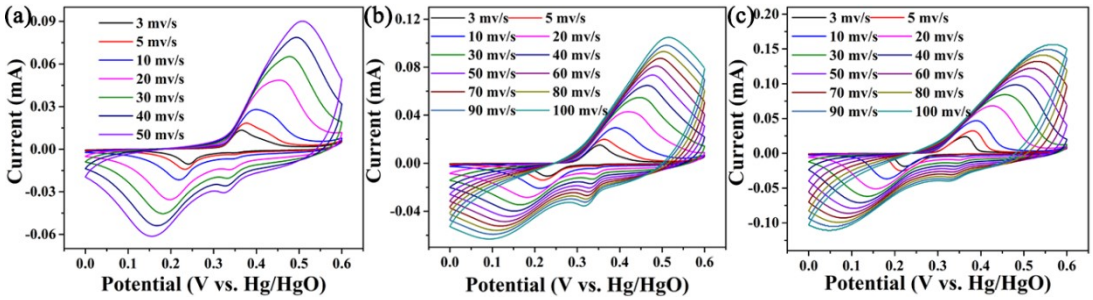

Figure S8. CV curves of (a) NiCo-LDH,(b) NiCo-LDH/rGO-1 and (c) NiCo-LDH/rGO-3 at different scan rates.

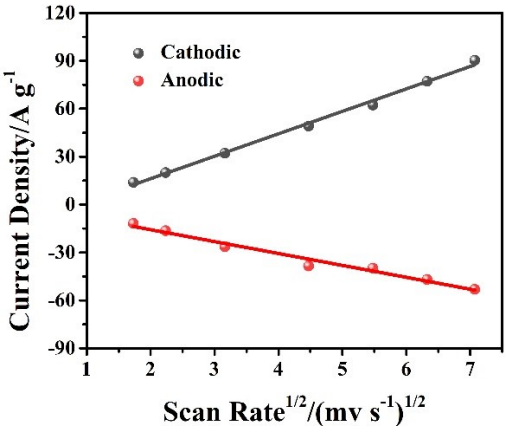

Figure S9. the linear relation between the anodic/cathodic peak currents and the scan rates.

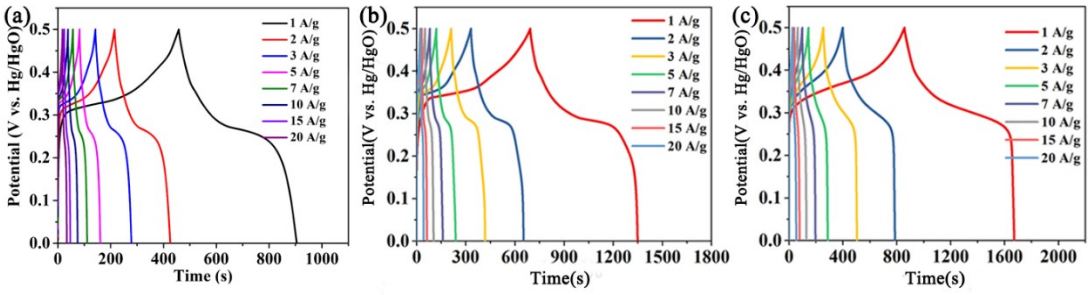

Figure S10. GCD plots of (a) NiCo-LDH,(b) NiCo-LDH/rGO-1 and (c) NiCo-LDH/rGO-3 at various current densities.

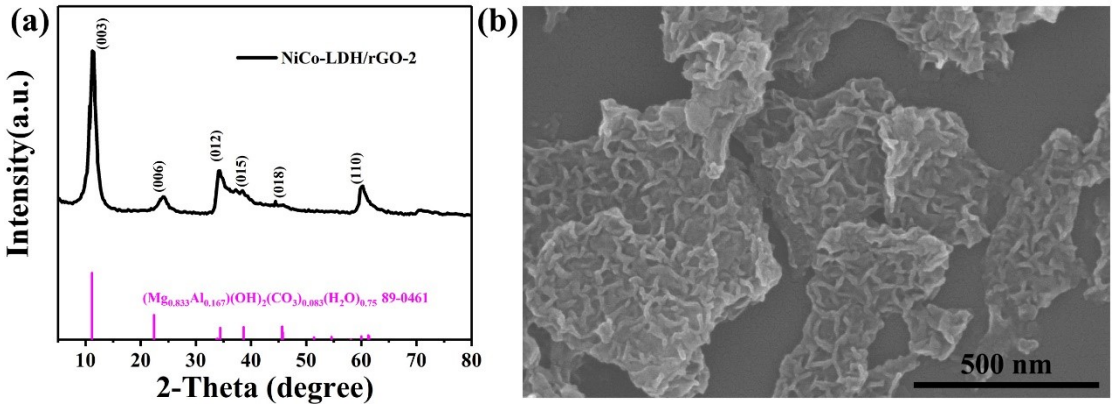

Figure S11. (a) XRD pattern of NiCo-LDH/rGO-2 after 4000 clcyes; (b) SEM image of NiCo-LDH/rGO-2 after 4000 clcyes

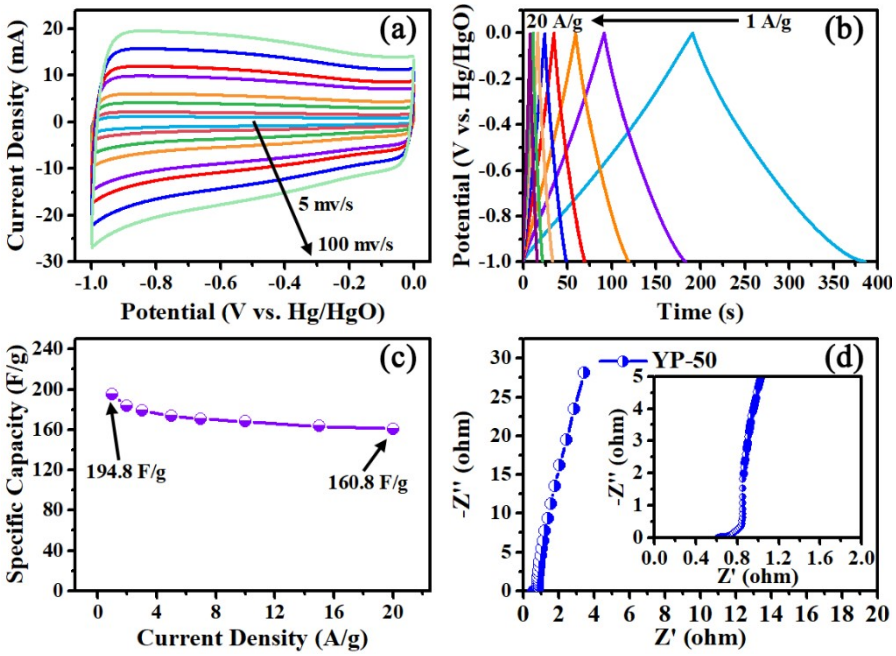

Figure S12. (a) CV curves of the YP-50 electrode at different scan rates from 5 to 100 mV s-1 (b) GCD plots of the YP-50 electrode at various current densities, (c) The corresponding specific capacitance of the YP-50 electrode at different discharge current densities. (d) Nyquist plots of the YP-50 electrode.

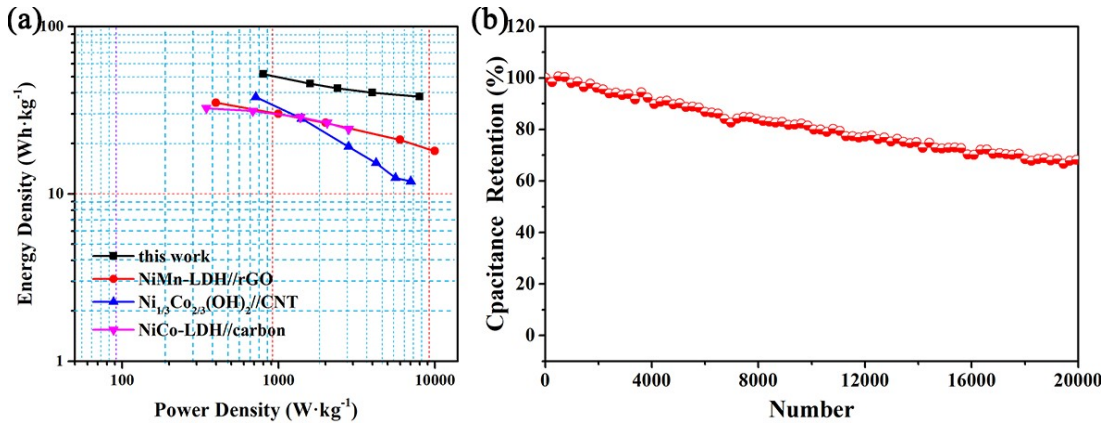

Figure S13. (a) Comparison in a Ragone plot of the energy densities and power densities reported in previous references and those of our NiCo-LDH/rGO-2//YP-50 ASC device. (b) Cycling stability of the ACS device.

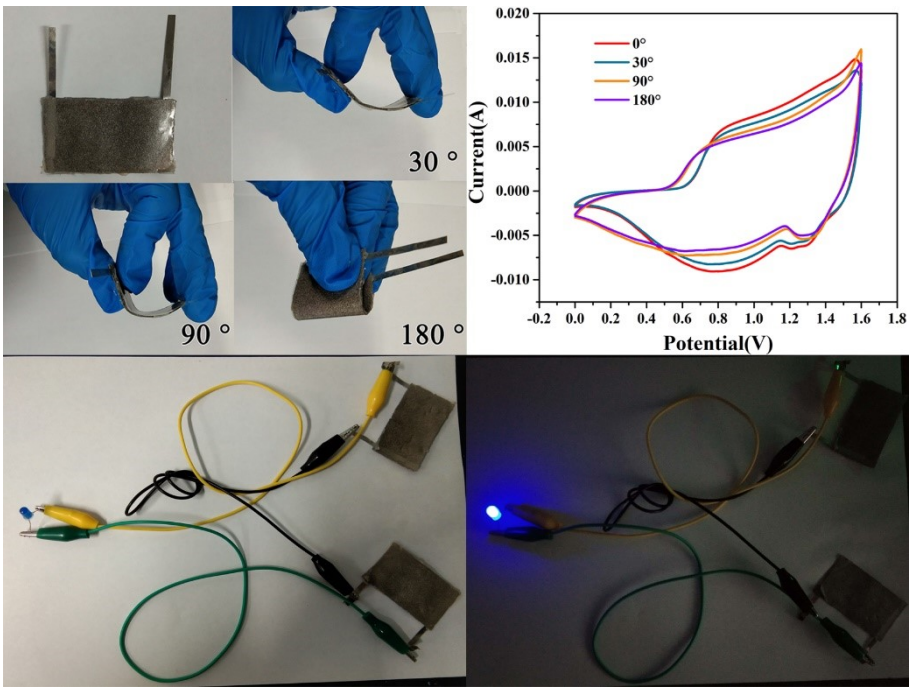

Figure S14. (a) Bending test of the ACS device;(b) CV cuvres of the ACS device under different bending angles; (c) (d) the photograph showing that two ACS devices in series can light up a red LED.